# Archaeal Membrane Lipid-Based Paleothermometry for Applications in Polar Oceans

By Susanne Fietz, Sze Ling Ho, and Carme Huguet

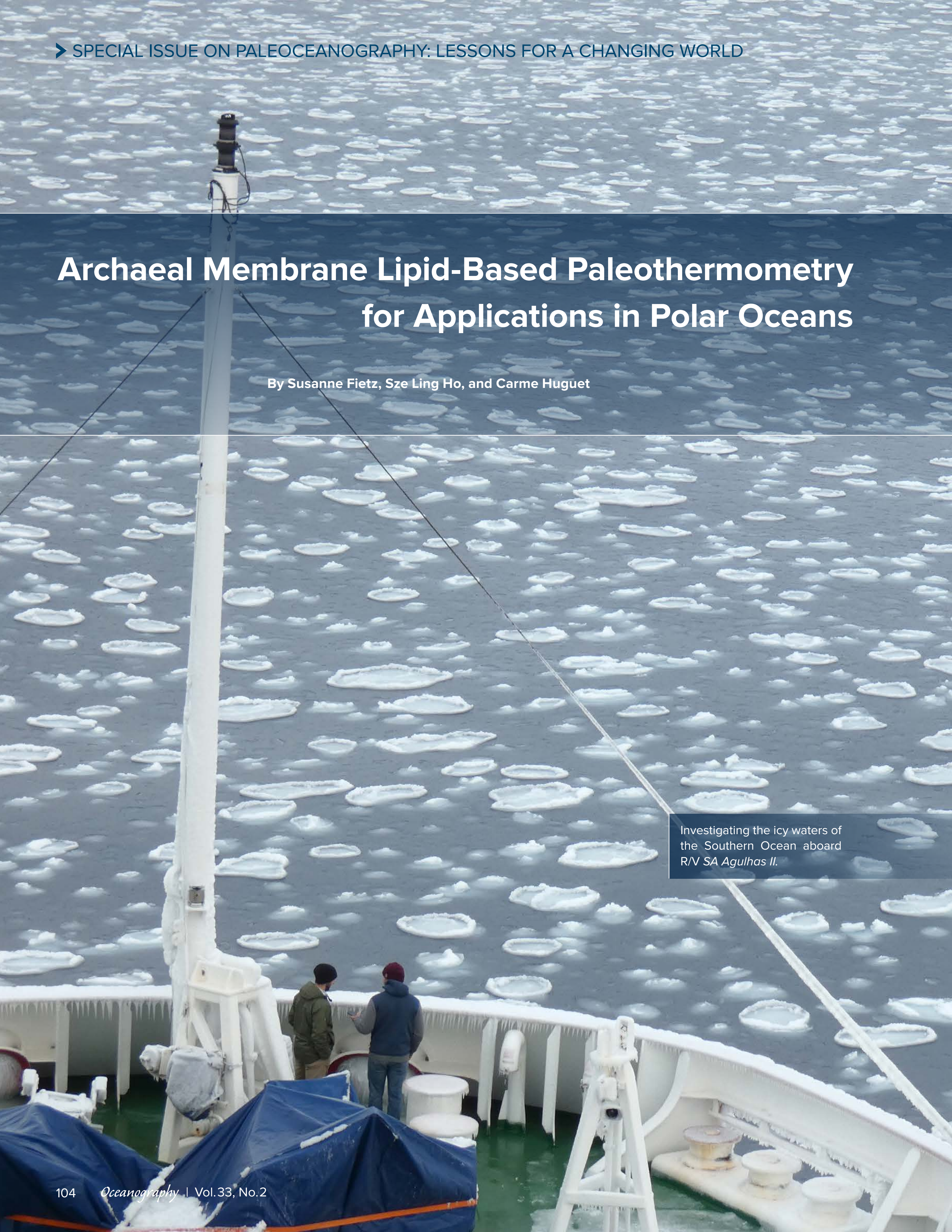

Investigating the icy waters of the Southern Ocean aboard R/V *SA Agulhas II*.

**ABSTRACT.** To establish whether ongoing climate change is outside the range of natural variability and a result of anthropogenic inputs, it is essential to reconstruct past oceanic and atmospheric temperatures for comparison with the modern world. Reconstructing past temperatures is a complex endeavor that employs indirect proxy indicators. Over the past two decades, promising paleothermometers have been developed that use isoprenoidal glycerol dialkyl glycerol tetraethers (isoGDGTs) from the membrane lipids of archaea preserved in marine sediments. These proxies are based on the observed relationship between lipid structure and temperature. As with all proxy indicators, observed relationships are often complex. Here, we focus on the application of isoGDGT paleotemperature proxies in the polar oceans, critical components of the global climate system. We discuss the application of and caveats regarding these archaeal membrane lipid-derived proxies and make recommendations to improve isoGDGT-derived polar ocean temperature reconstructions. We also review initial successes using hydroxylated (OH) isoGDGTs proxies in cold Arctic and Southern Ocean regions and recommend that multi-proxy approaches, including both hydroxylated and non-hydroxylated isoGDGTs, be used to contribute to the robustness of paleotemperature reconstructions.

## INTRODUCTION

Given the rate and societal impact of ongoing human-caused warming, understanding the geographical extent, magnitude, and frequency of past global climate variations is essential. Ocean temperature is a critical parameter in the climate system. While sea surface temperature reflects heat exchange between the ocean and atmosphere, as well as large-scale ocean circulation, the average temperature of the upper ocean (0–1,000 m) is a useful estimate of upper ocean heat content. Thus, a top priority in paleoceanography is to provide accurate proxy-based ocean temperature reconstructions across all timescales (millions to hundreds of years). This information, gleaned from geological records, is essential for validating numerical models used to project future change and to inform policymakers who are developing strategies for mitigation and adaptation.

Efforts to reconstruct past surface and bottom water temperatures have expanded to include the polar regions (e.g., Shevenell et al., 2011; Fietz et al., 2016), where reliable instrumental temperature data are only available for the past 100 years (e.g., Hansen et al., 2010; IPCC, 2019, and references therein). Part of the impetus for this focus is the revelation that retreating grounding lines accompanied by warming ocean waters are resulting in Antarctic ice sheet mass loss and global sea level rise (Jacob et al., 2012; Rintoul et al., 2018). Furthermore, the Intergovernmental Panel on Climate Change states with high confidence that "both polar oceans have continued to warm in recent years, with the Southern Ocean being disproportionately and increasingly important in global ocean heat increase" (IPCC, 2019).

As calcium carbonate microfossils are not always continuously preserved in high-latitude sediments (e.g., Zamelczyk et al., 2012), paleoceanographers turn to non-carbonate-based molecular fossils to determine past variations in high-latitude ocean water temperatures (e.g., Sluijs et al., 2006; Bijl et al., 2009; Shevenell et al., 2011). Lipids preserved in marine sediments that have been successfully used in paleotemperature reconstructions include algal alkenones and archaeal isoprenoidal glycerol dialkyl glycerol tetraethers (isoGDGTs), which are sensitive to temperature change and relatively resilient to degradation compared to other lipids (e.g., Huguet et al. 2008; Zonneveld et al., 2010; Schouten et al., 2013; Herbert, 2014, and references therein). For example, the most mature of these paleothermometers, the alkenone unsaturation index $U^{K'}_{37}$, was developed in 1986 (Brassell et al., 1986) and is widely used to reconstruct sea surface temperatures (e.g., Ho et al., 2013; Herbert, 2014, and references therein). Subsequently, the archaeal isoGDGT-based paleotemperature proxy known as the TetraEther indeX of 86 carbons, $TEX_{86}$, was proposed (Schouten et al., 2002) and well received by the organic geochemistry community.

One advantage of proxies that employ archaeal membrane lipids is that these molecules are ubiquitous in globally distributed marine sediments, making them useful for calibration and estimating low-to-high latitude thermal gradients (Schouten et al., 2002). However, as with all proxies, researchers have discovered a number of non-thermal factors that affect the distribution of isoGDGTs in marine sediments. Because archaea occupy almost every niche on Earth, a number of studies have been undertaken to improve our understanding of archaeal distribution, ecophysiology (e.g., Hayes, 2000), and membrane molecular structure (e.g., Chugunov et al., 2015).

Here, we review current knowledge of the archaeal isoGDGT paleotemperature proxies, including the recent hydroxylated isoGDGT (OH-isoGDGTs) paleothermometer. We focus our review on recent insights gained from using these archaeal membrane lipid paleothermometers in the polar regions.

## ARCHAEAL MEMBRANE LIPIDS AND PALEOTHERMOMETRY

Membranes are the interfaces between (micro)organisms and their environments. The key roles they play in metabolism (e.g., providing energy to the cell using ion gradients across the membranes; Konings et al., 2002; Zhou et al., 2020) and environmental sensing and signaling (Ren and Paulsen, 2005) require constant composition adjustments (Oger and Cario, 2013). Archaea synthesize tetraether lipids that span the entire membrane and form a monolayer (Koga and Morii, 2007). The isoGDGTs are a subset of these archaeal tetraether lipids, and their composition is group specific; for example, Thaumarchaeota preferentially synthesize isoGDGTs with cyclopentane rings (Sinninghe Damsté et al., 2002). Archaea also produce OH-isoGDGTs (Lipp and Hinrichs, 2009) that were first discovered in methanotrophic archaea (Hinrichs et al., 1999) and later in Thaumarchaeota (Elling et al., 2017; Bale et al., 2019).

The stability of archaeal membranes increases with ambient growth temperature, especially in thermophilic extremophiles (De Rosa et al., 1980). Yet, it was not until the 2000s that geochemists exploited this observation to develop quantitative temperature proxies (e.g., Schouten et al., 2002; Kim et al. 2010; Ho et al., 2014; Tierney and Tingley, 2014). Of particular importance for understanding isoGDGT-based proxies is that, at all temperatures, archaea must maintain semi-permeability without impacting rigidity (e.g., Chugunov et al., 2015). Most isoGDGTs involved in paleothermometry contain one or more cyclopentane rings, resulting in tighter packing and a more stable membrane (see Figure 1 in Zhou et al., 2020). At low temperatures, archaea reduce the number of cyclopentane rings in their membrane structures, thereby preventing membrane rigidity (Gabriel and Chong, 2000; Schouten et al., 2002). Indeed, Schouten et al. (2002) observed that the cyclization of isoGDGTs in surface marine sediments is correlated globally with measured surface water temperature in mesophilic (non-extreme) environments, resulting in the development of the first archaeal lipid paleothermometer, $TEX_{86}$ (Table 1). In addition, in Thaumarchaeota, hydroxylation increases membrane fluidity and transport (Huguet et al., 2017), which compensates for increased rigidity at lower temperatures. The observation that the number of rings in hydroxylated isoGDGTs changes with temperature led to the development of ring-number-based OH-isoGDGT proxies (Fietz et al., 2013; Lü et al., 2015; Table 1).

## $TEX_{86}$ RECONSTRUCTIONS IN POLAR OCEANS: OPPORTUNITIES AND CHALLENGES

The general relationship between the number of rings in sedimentary GDGTs and the overlying mean annual sea surface temperature is that the warmer the seawater, the more isoGDGTs there are with higher numbers of cyclopentane rings (e.g., isoGDGT-2 and isoGDGT-3), resulting in higher $TEX_{86}$ index values; incorporation of the isomer of crenarchaeol adds accuracy (Sinninghe Damsté et al., 2002). Kim et al. (2010) proposed a variant of $TEX_{86}$, termed $TEX^{L}_{86}$, that employs a different GDGT combination ($TEX^{L}_{86}$; Table 1) and is intended for temperatures below 15°C.

The isoGDGT-derived indices in surface sediments are generally well correlated with seawater temperatures in the overlying upper water column (e.g., Kim et al., 2010; Ho et al., 2014; Tierney and Tingley, 2014; Figure 1). In global calibrations, the standard errors of temperature estimates vary between 4.0°C and

**TABLE 1.** Isoprenoid and hydroxylated GDGT-derived indices proposed for paleotemperature estimates. In the equations, the abbreviation GDGT*n* represents isoGDGTs with *n* number of cyclopentane rings. For example, isoGDGT-1 represents the non-hydroxylated isoprenoid GDGT with one cyclopentane moiety. The abbreviation OH-isoGDGT*n* stands for hydroxylated isoprenoid GDGTs with *n* number of cyclopentane rings. The term ΣisoGDGTs refers to the sum of all non-hydroxylated isoprenoid GDGTs (e.g., isoGDGT-1, isoGDGT-2, isoGDGT-3, crenarchaeol and its isomer, abbreviated in this table as cren'). The term ΣOH-isoGDGTs refers to the sum of OH-isoGDGT-0, OH-isoGDGT-1 and OH-isoGDGT-2.

| INDEX | EQUATION | REFERENCE |
|---|---|---|
| $TEX_{86}$ | $\frac{[isoGDGT-2]+[isoGDGT-3]+[cren']}{[isoGDGT-1]+[isoGDGT-2]+[isoGDGT-3]+[cren']}$ | Schouten et al., 2002 |
| $TEX^{L}_{86}$ | $\log\left(\frac{[isoGDGT-2]}{[isoGDGT-1]+[isoGDGT-2]+[isoGDGT-3]}\right)$ | Kim et al., 2010 |
| OH−GDGT% | $\frac{\Sigma OH-isoGDGTs}{(\Sigma OH-isoGDGTs+\Sigma isoGDGTs)}\times 100$ | Huguet et al., 2013 |
| $OH-GDGT_{1318/1316}$ | $\frac{OH-isoGDGT-0}{OH-isoGDGT-0+OH-isoGDGT-1}$ | Fietz et al., 2013 |
| RI-OH | $\frac{[OH-isoGDGT-1]+2\times[OH-isoGDGT-2]}{[OH-isoGDGT-0]+[OH-isoGDGT-1]+[OH-isoGDGT-2]}$ | Lü et al., 2015 |
| RI-OH' | $\frac{[OH-isoGDGT-1]+2\times[OH-isoGDGT-2]}{[OH-isoGDGT-1]+[OH-isoGDGT-2]}$ | Lü et al., 2015 |
| $OH^{c}$ | $\frac{[isoGDGT-2]+[isoGDGT-3]+[cren']-[OH-isoGDGT-0]}{[isoGDGT-1]+[isoGDGT-2]+[isoGDGT-3]+[cren']+\Sigma OH-isoGDGTs}$ | Fietz et al., 2016 |

5.2°C for $\mathrm{TEX}^{L}_{86}$ and $\mathrm{TEX}_{86}$, respectively (Kim et al., 2010). Interlaboratory error (3°–4°C) for $\mathrm{TEX}_{86}$ are the same order of magnitude as other commonly used quantitative temperature proxies (Schouten et al., 2013). There is, however, a larger scatter in the $\mathrm{TEX}_{86}$–sea surface temperature (SST) relationships at the low temperature end of the calibrations (Figure 1; Kim et al., 2010; Ho et al., 2014; Tierney and Tingley, 2014). The scatter is partly due to bias from terrestrial input, especially in the Arctic Ocean (Ho et al., 2014; Y. Park et al., 2014), and potentially from the use of satellite-assigned sea surface temperatures below the seawater freezing point for some calibrations (Pearson and Ingalls, 2013). Large scatter in $\mathrm{TEX}_{86}$–SST relationship is not an issue unique to the polar oceans. It also exists at the high-temperature end in the Red Sea (Figure 1), likely due to an endemic Thaumarchaeota population (Trommer et al., 2009). As such, $\mathrm{TEX}_{86}$ and its variants may be affected by environmental conditions other than temperature, such as pH (Elling et al., 2015), oxygen availability (Qin et al., 2015), cellular physiological acclimation including ammonia oxidation rates (Elling et al., 2014; Hurley et al., 2016), and shifts in season and depth of production (Huguet et al., 2007; Ho and Laepple, 2016; Chen et al., 2018). Many of the caveats mentioned above have been reviewed for the global ocean in general (see, for example, comprehensive reviews by Pearson and Ingalls, 2013; Schouten et al., 2013; and Tierney, 2014). Figure 2 illustrates concerns raised for the polar oceans.

A solution for overcoming some of the caveats is to develop a regional calibration. For instance, Shevenell et al. (2011) applied a regionally calibrated $\mathrm{TEX}_{86}$ equation instead of $\mathrm{TEX}^{L}_{86}$ to reconstruct Holocene temperature evolution in the Antarctic Peninsula (Figure 1a). Some sources of uncertainty, such as spatial change in the archaeal community, cannot be included in ordinary least squares regression approaches for global calibration. Thus, alternative statistical approaches have also been adopted to improve correlation of $\mathrm{TEX}_{86}$ with upper ocean temperature, such as Bayesian regression (BAYSPAR; Tierney and Tingley, 2014) and machine-learning approaches (OPTiMAL; Eley et al., 2019).

Despite calibration challenges, inherent to all paleotemperature proxies, the $\mathrm{TEX}_{86}$ paleothermometer revolutionized understanding of past ocean temperature changes in the carbonate-poor polar regions. In the Arctic Ocean, $\mathrm{TEX}_{86}$ provided one of the first quantitative temperature estimates for past warm climates characterized by high atmospheric $CO_2$, such as the Cretaceous and the Eocene. $\mathrm{TEX}_{86}$ revealed that the Arctic surface ocean during these time peri-

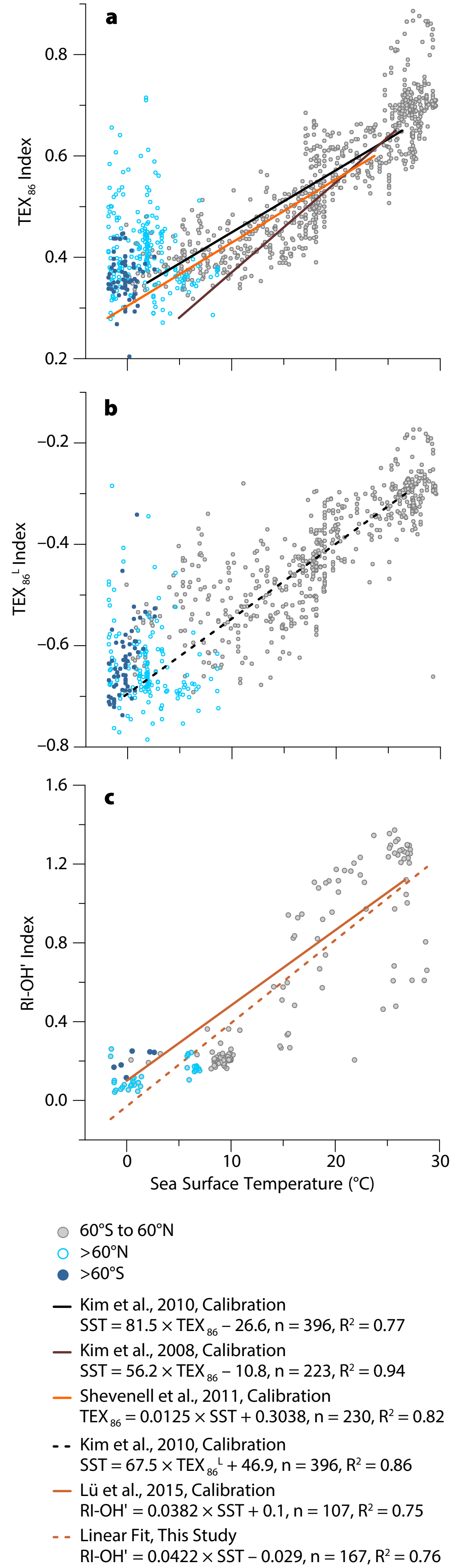


**FIGURE 1.** Selected global calibrations for paleothermometers (a) $\mathrm{TEX}_{86}$ (TetraEther indeX of 86 carbons), (b) $\mathrm{TEX}^{L}_{86}$ (which employs a different combination of glycerol dialkyl glycerol tetraethers from $\mathrm{TEX}_{86}$ and is intended for temperatures below 15°C), and (c) RI-OH' (the weighted average number of cyclopentane rings) against sea surface temperatures. The data for the scatterplots in (a) and (b) are sourced from Tierney and Tingley (2015). A new, extended compilation of published data sets is presented here for RI-OH' (Fietz et al., 2013; Huguet et al., 2013; Lü et al., 2015; Kaiser and Arz, 2016). In (c), linear plots illustrate published calibrations for all three indices as well as a new linear fit for the extended RI-OH' data set.

ods was as warm as today's subtropics, a stark contrast to the currently ice-covered Arctic (e.g., Jenkyns et al., 2004; Brinkhuis et al., 2006; Sluijs et al., 2006). Similarly, in the Southern Ocean, $TEX_{86}$ and its variants have made it possible to reconstruct the temperature evolution from the Jurassic to the Holocene (summarized in Table 2). Thanks to this large body of work, we now know that the surface temperature of the Southern Ocean was once as high as 30°C during the Jurassic (Jenkyns et al., 2012) and has cooled through the Cenozoic, resulting in present-day temperatures surrounding the Antarctic Peninsula (Shevenell et al., 2011; Etourneau et al., 2013). Importantly, $TEX_{86}$-based reconstructions have helped characterize past greenhouse climates, suggesting that Antarctic surface water temperatures were >10°C during the Early Eocene Climatic Optimum (e.g., Bijl et al., 2009). These reconstructions also improved understanding of temperature magnitude ranges over major climate transitions, including the >4°C cooling across the Eocene-Oligocene transition (e.g., Bijl et al., 2009; Z. Liu et al., 2009). $TEX_{86}$-based paleotemperature studies also indicate that in climatically sensitive regions, surface ocean temperatures fluctuated abruptly during the Holocene (Shevenell et al., 2011), suggesting the potential for rapid polar ocean temperature fluctuations with continued warming. Furthermore, both long-term cooling and millennial-scale variability on the western Antarctic Peninsula are similar to changes in the low latitudes (i.e., the tropical Pacific) and in regional ice core records (Mulvaney et al., 2012), suggesting climate teleconnections between the low and high latitudes via the Southern Hemisphere westerlies (Shevenell et al., 2011).

## DOES INCLUDING OH-isoGDGTs IN TEMPERATURE PROXY INDEX IMPROVE THE ESTIMATES?

At some sites in the Arctic and Southern Oceans, $TEX_{86}$ and $TEX^{L}_{86}$ do not show expected changes. For example, analyses using these proxies do not reflect the warmer conditions during glacial retreat in the Pliocene Arctic (Knies et al., 2014), during the Plio-Pleistocene transition and Pleistocene deglaciations in the Southern Ocean (e.g., McKay et al., 2012; Fietz et al., 2016), and during the late Holocene Arctic sea ice melting (e.g., Fietz et al., 2013). Some inconsistencies in warmer reconstructed temperatures during the deglacials compared to peak interglacials may be attributed to increased meltwater stratification (Shevenell et al., 2011; McKay et al., 2012). Another caveat of particular importance here is the potential lack of $TEX_{86}$ sensitivity at tempera-

| CAVEATS POTENTIALLY ENCOUNTERED IN THE POLAR OCEANS | SOLUTIONS |
|---|---|
| **Calibration Issues**<br>Calibration does not perform well at low temperature end (i.e., at high latitudes)[1,2,3] | • Use different isoGDGT index[1] or calibration<br>• Including OH-isoGDGTs in toolkit may improve temperature reconstructions[e.g., 4,5] |
| **Terrestrial Input**<br>Deviation from expected seawater temperature especially in the Arctic[e.g., 6, 7] | • Monitor relative terrestrial input, e.g., using BIT[8]<br>• OH-isoGDGTs may help, but contradictory findings exist on the effect of terrestrial input on OH-isoGDGT distribution[e.g., 9,10,11,12] |
| **Different Ecotypes**<br>Studies report different ecotypes, e.g., in the Red Sea[13]; suspected also in the polar oceans | • Regional calibration, e.g., for the Antarctic Peninsula[14] |
| **Depth Origin of the Sedimentary Signal**<br>Subsurface origin reported in several environments, including in the polar oceans[1,15] | • Test subsurface calibrations[20]<br>• Be aware where this may be an issue |
| **Physiological Effects**<br>Culture studies reported evidence for and against non-thermal effects on cyclization[e.g.,16,17]; no polar specific cultivates yet, but results may apply everywhere | • No definite solution yet<br>• Be aware that it may be an issue when interpreting data |
| **Production and Reworking in Sediment**<br>Impact by sedimentary production, e.g., by methanotrophs, methanogens[18,19]; more likely to affect deep-time records in polar oceans | • Test for Methane and Ring Indices to detect atypical isoGDGT distributions[18] |

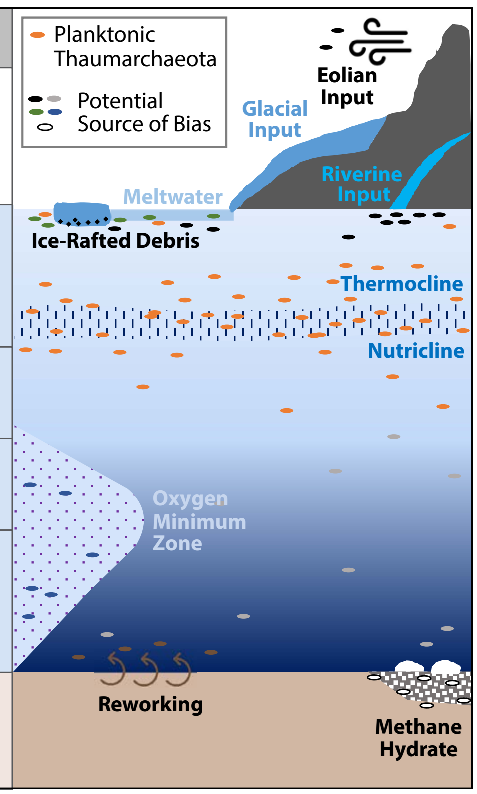


FIGURE 2. Overview of processes in the water column that can bias the isoprenoidal glycerol dialkyl glycerol tetraether (isoGDGT)-based paleotemperature reconstruction, especially in the polar oceans. Recommendations on how to work with such caveats and how including hydroxylated isoGDGTs (OH-isoGDGTs) in the paleothermometry toolbox may help are included. [1]Kim et al. (2010), [2]Ho et al. (2014), [3]Tierney and Tingley (2014), [4]Fietz et al. (2013), [5]Fietz et al. (2016), [6]Ho et al. (2014), [7]Y. Park et al. (2014), [8]Hopmans et al. (2004), [9]Kaiser and Arz (2016), [10]Lü et al. (2019), [11]Kang et al. (2017), [12]Wei et al. (2019), [13]Ionescu et al. (2009), [14]Shevenell et al. (2011), [15]Huguet et al. (2007), [16]Wuchter et al. (2004), [17]Qin et al. (2015), [18]Zhang et al. (2016), [19]Shah et al. (2008), [20]Ho and Laepple (2016).

tures below 10°C as observed in mesocosms studies (e.g., Wuchter et al., 2004). In cold waters, archaea adjust the permeability of their membranes by changing the number of rings and adding hydroxyl groups. Including only one of the processes in the proxy index may therefore underestimate the full range of temperature acclimations of archaea in polar oceans. Hence, accounting for both processes by adding OH-isoGDGTs to the paleothermometer index should, in principle, improve the sensitivity of the proxy.

Like isoGDGTs, OH-isoGDGTs are globally distributed in the water column and in sediments (X.-L. Liu et al., 2012; Huguet et al., 2013; Figure 3). X.L. Liu et al. (2012) suggested that OH-isoGDGTs had potential for paleothermometry, and Huguet et al. (2013) proposed the first OH-isoGDGTs-based temperature proxy after observing a strong correlation between the relative abundance of OH-isoGDGTs and sea surface temperatures in globally distributed seawater and sediment samples. Thereafter, several indices were proposed for applications in the polar oceans (Table 1). While the addition of hydroxylated isoGDGTs in the isoGDGT toolbox was originally proposed as an alternative for cold water paleothermometry (e.g., Fietz et al., 2013; Huguet et al., 2013), it was later suggested that an OH-isoGDGT-temperature relationship also exists globally (Lü et al., 2015). The finding of OH-isoGDGTs in a large set of surface sediments in Chinese coastal seas (n = 70; Figure 3) led Lü et al. (2015) to propose the weighted average number of cyclopentane rings (RI-OH index) as a proxy for sea surface temperatures, as well as a polar variant, the RI-OH' (Table 1; Figure 1c), with a residual standard error of 6.0°C (compared to 5.2°C for $TEX_{86}$; Kim et al., 2010). This RI-OH index reasonably reproduced $TEX_{86}$-derived temperatures dating back 30–40 million years for the US New Jersey shelf (de Bar et al., 2019).

Thus far, OH-isoGDGT-based proxies have been applied to Arctic and Southern Ocean sediments to reconstruct seawater temperatures and to help elucidate ice-ocean dynamics (Fietz et al., 2013, 2016; Knies et al., 2014; Kremer et al., 2018). In these cases, OH-isoGDGT proxies were utilized instead of $TEX_{86}$ as the latter did not yield changes in accordance with other proxies (Figure 4). For example, in Fram Strait, the gateway to the Arctic Ocean, the OH-isoGDGT-derived indices indicated sea surface cooling of ~5°C (OH-isoGDGT%) and ~3°C (RI-OH') across the Plio-Pleistocene transition, suggesting an increasing influence of polar water masses (Knies et al.,

**TABLE 2.** isoGDGT-inferred Jurassic-Holocene upper ocean temperature evolution in the Southern Ocean.

| TIME PERIOD STUDIED | GDGT INDEX | MAIN FINDING IN TERMS OF TEMPERATURE CHANGE | REFERENCE |
|---|---|---|---|
| Jurassic-Cretaceous | $TEX_{86}$ | Persistent high temperatures of 26°–30°C[a] | Jenkyns et al., 2012 |
| Eocene | $TEX_{86}$ | Cooling from ~25°C during early Eocene to ~21°C during late Eocene[b] | Bijl et al., 2009 |
| Eocene-Oligocene | $TEX_{86}$ | Substantial cooling of >5°C across the Eocene-Oligocene boundary | Z. Liu et al., 2009 |
| Oligocene-Miocene | $TEX_{86}$ | ~5°–6°C cooling from Oligocene to mid-Miocene | Hartman et al., 2018 |
| Miocene | $TEX^L_{86}$ | Cold (–1°–3°C) and warm (6°–10°C) intervals during early to mid Miocene[c] | Levy et al., 2016 |
| Miocene | $TEX^L_{86}$ | ~14°C before the mid-Miocene climatic optimum, and ~8°C thereafter[c] | Sangiorgi et al., 2018 |
| Pliocene | $TEX^L_{86}$ | Cooling, from ~5°C during early Pliocene to ~2°C during the late Pliocene[d] | McKay et al., 2012 |
| Pleistocene | $TEX^L_{86}$ | ~5°C warming from glacial to deglaciation | Hayes et al., 2014 |
| Last Glacial-Holocene | $TEX_{86}$ | Warming from ~10°C during the last glacial to ~19°C during the early Holocene[b] | Kim et al., 2009 |
| Holocene | $TEX^L_{86}$ | ~3°C of cooling over the Holocene | Etourneau et al., 2013 |
| Holocene | $TEX_{86}$ | 3°–4°C of cooling over the past 12,000 years; superimposed series of millennial-scale warm and cold events | Shevenell et al., 2011 |
| Holocene | $TEX^L_{86}$ | No long-term trend over the Holocene | Kim et al., 2012 |
| Holocene | $TEX^L_{86}$ | Abrupt warming of ~1.5°C in the early Holocene, possibly associated with ice shelf disintegration | Etourneau et al., 2019 |

[a] 5.2°C standard error of the estimate for $TEX_{86}$ (Kim et al., 2010)
[b] 1.7°C standard error of the estimate for $TEX_{86}$ (Kim et al., 2008)
[c] 2.8°C standard error of the estimate for $TEX^L_{86}$ (Kim et al. 2012)
[d] 4.0°C standard error of the estimate for $TEX^L_{86}$ (Kim et al. 2010)

2014). In contrast, $TEX^{L}_{86}$ temperatures did not reveal consistent temporal patterns. Meanwhile, a reconstruction over the past ~120,000 years (Kremer et al., 2018) revealed more reasonable RI-OH'-inferred temperatures (–2.5° to 2.5°C; calibration error of 6°C) than $TEX^{L}_{86}$-derived temperatures (–17° to 9°C; calibration error of 4°C). Over the Holocene, temperatures based on the OH-isoGDGT% and RI-OH' indices also followed trends in temperature and water mass changes indicated by multiple proxies, in contrast to the $TEX^{L}_{86}$-based temperatures (Fietz et al., 2013; Figure 4).

The reasons for the mismatch between $TEX_{86}$-related temperatures and other proxies in the Arctic are unknown. The isoGDGT-based Ring Index (Zhang et al., 2016) may shed light on the extent of non-thermal bias of the $TEX_{86}$-related reconstructions, especially potential terrestrial input. Ring Index offset values lower than 0.3 at the Plio-Pleistocene transition (Knies et al., 2014) and in the Holocene (Fietz et al., 2013) do not point to a specific non-thermal bias. The factors driving the mismatch between $TEX_{86}$-related temperatures and other proxies in the Arctic do not seem to affect the utility of OH-isoGDGT proxies, as the reconstruction based on them coevolves with other temperature proxies (Figure 4).

The OH-isoGDGT proxy has not been widely tested in the Southern Ocean. E. Park et al. (2019) recently published the very first sediment trap-based study indicating that several OH-isoGDGT-based proxies show promise as temperature proxies for both the Arctic and the Southern Oceans. To date, only one study has applied the OH-isoGDGTs for reconstructions in the Southern Ocean (Fietz et al., 2016). Here, in the subantarctic Atlantic, $TEX_{86}$ (Figure 3) suggests warmer conditions during glacials than interglacials in the past 500,000 years, in contrast to other paleotemperature proxies based on the same sediment core (Fietz et al., 2016). Located north of the winter sea ice extent during the last glacial maximum, some inconsistencies of warmer reconstructed temperatures during the glacial and colder temperatures during the interglacial may be attributed to increased meltwater stratification (Shevenell et al., 2011; McKay et al., 2012). Another possible explanation for the "warm" glacial $TEX_{86}$-temperatures in the subantarctic Atlantic record

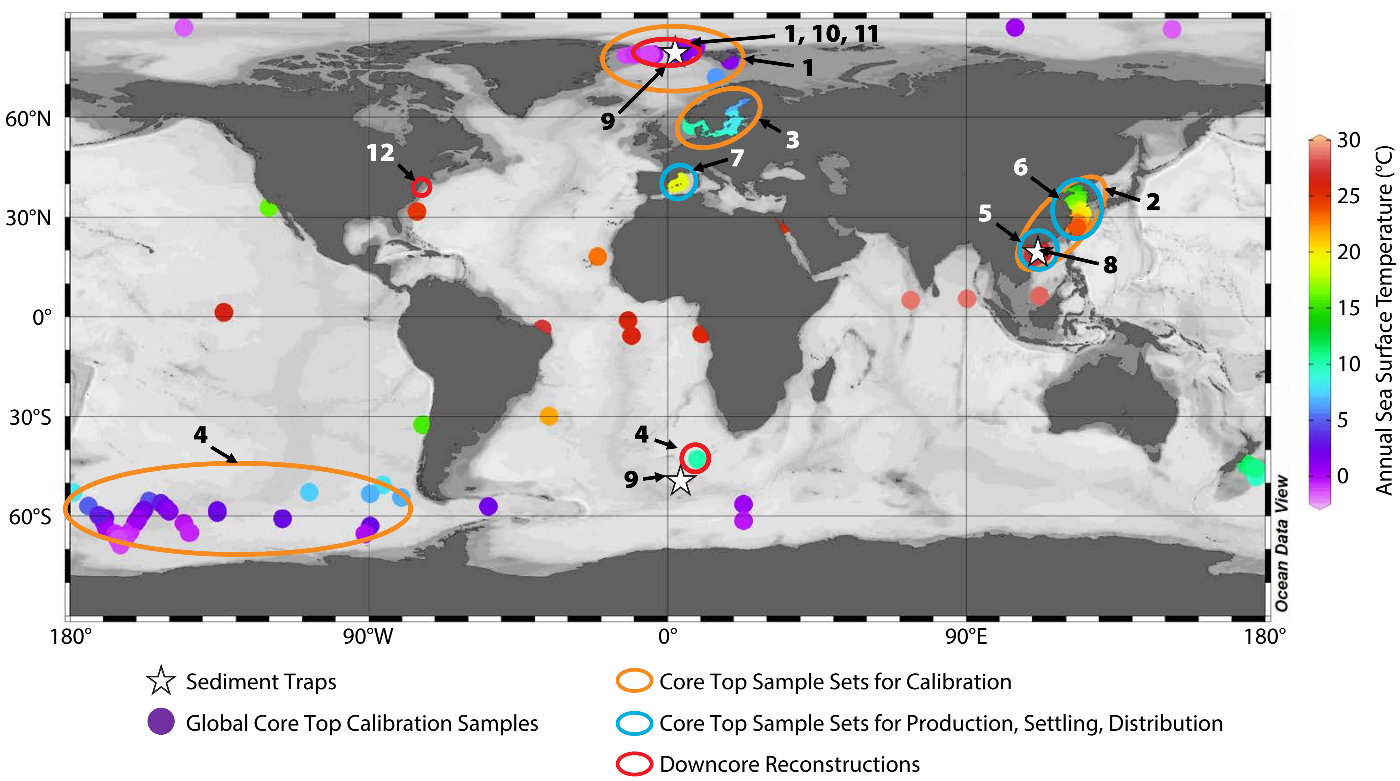


**FIGURE 3.** An Ocean Data View (Schlitzer, 2018) map illustrates the progress made since the OH-isoGDGTs were first proposed in 2013 as paleotemperature proxies, including surface sediment sample locations used for calibrations of initial OH-isoGDGT% (unlabeled filled circles; Huguet et al., 2013). Orange circles roughly indicate the locations of the additional sample sets for calibrations of cyclization variants, such as $OH\text{-}isoGDGT_{1318/1316}$ (Table 1) by Fietz et al. (2013, #1), RI-OH and RI-OH' (Table 1) by Lü et al. (2015; #2), and improved calibrations thereof by Kaiser and Arz (2016; #3), as well as for $OH^{c}$ index determination (Table 1) by Fietz et al. (2016; #4). Blue circles highlight focus areas of surface sediment studies that improve our understanding of OH-isoGDGT production, settling, and thus ultimately, distribution in the sediment (#5, Lü et al., 2019; #6, Kang et al., 2017; #7, Davtian et al., 2019). White stars indicate two sediment trap studies (#8, Wei et al., 2019, South China Sea; #9, E. Park et al., 2019, Fram Strait and Southern Ocean). Red circles roughly indicate downcore temperature reconstructions (#1, Fietz et al., 2013; #10, Knies et al., 2014; #4, Fietz et al., 2016; #11, Kremer et al., 2018; #12, de Bar et al., 2019). Circles and stars are not to scale and may not represent 100% of the data set.

could be the bias toward warmer $TEX_{86}$-temperatures caused by low ammonium oxidizing rates (Hurley et al., 2016). However, higher eolian iron input during the glacials (Martinez-Garcia et al., 2009) would contribute to increased oxidation rates (Shafiee et al., 2019) and thus toward a cold bias of the $TEX_{86}$ temperatures and vice versa in the interglacials. This is the opposite of the temporal patterns in the $TEX_{86}$ records and, hence, a bias introduced by such nutrient dynamics does not explain the warm temperatures reconstructed during the glacials.

Adding OH-isoGDGTs in the temperature index improves the reconstruction to some degree. Unlike their counterparts $TEX_{86}$ and $TEX^{L}_{86}$, the OH-isoGDGT indices exhibit temporal patterns that are more consistent with other non-isoGDGT-based proxies (Figure 4) and expectations (lower temperatures during glacials), with the $OH^{c}$ index showing the best match in the temporal trend. In the

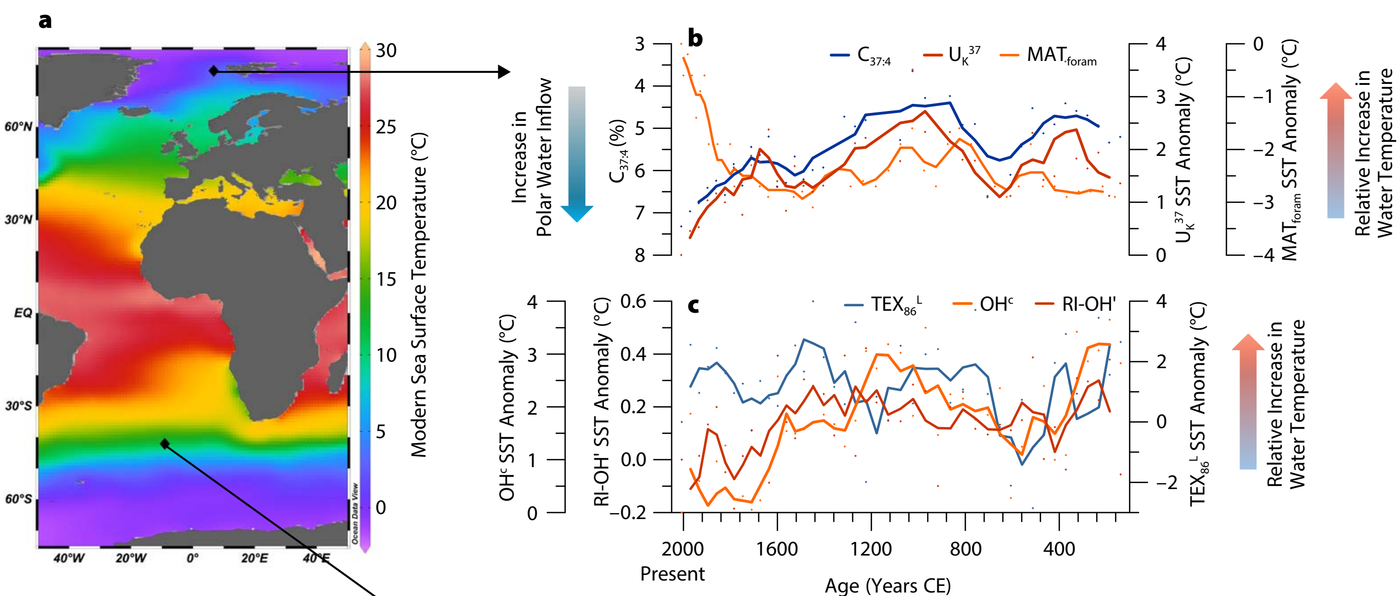


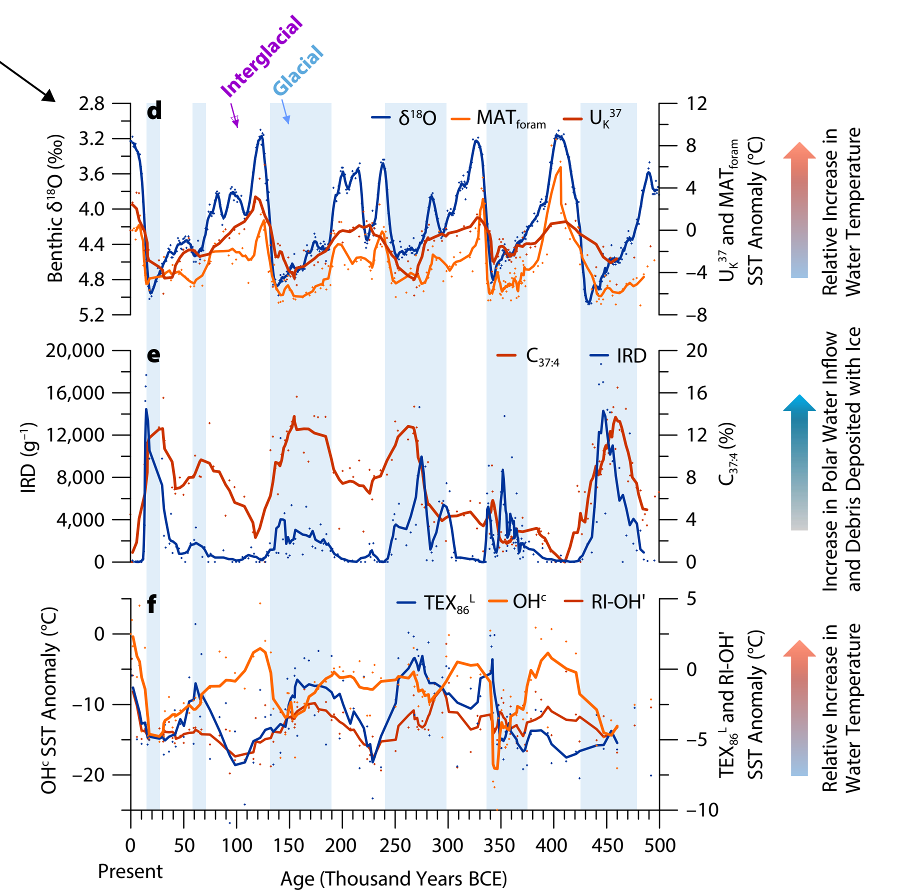


**FIGURE 4.** Multi-proxy based reconstructions of sea surface temperature and related parameters in the polar oceans. (a) Modern annual mean sea surface temperatures (from WOA2013, Locarnini et al., 2013). Black diamonds indicate the two sediment core sites in the Arctic (b–c) and Atlantic Southern Ocean (d–f). (b) Relative abundance of $C_{37:4}$ alkenones and $U^{K}_{37}$ sea surface temperature (SST) anomalies (Rueda et al., 2013) as well as SST anomalies reconstructed using modern analogue technique ($MAT_{foram}$-SST, Spielhagen et al., 2011). (c) $TEX_{86}$-, $TEX^{L}_{86}$-, and RI-OH'-derived SST anomalies using calibrations in Kim et al. (2010) and Lü et al. (2015), as well as $OH^{c}$-derived SST using calibration in Fietz et al. (2016). (d) Benthic $\delta^{18}O$ stack (Lisiecki and Raymo, 2005), summer SST (SSST) anomalies reconstructed using the modern analogue technique ($MAT_{foram}$-SSST; Becquey and Gersonde, 2002) and $U^{K}_{37}$ SST anomalies (Martinez-Garcia et al., 2009). (e) Relative abundance of $C_{37:4}$ alkenones to total $C_{37}$ alkenones, indicating cold water mass influence (Martinez-Garcia et al., 2009) and ice rafted debris (IRD) concentration (Becquey and Gersonde, 2002). (f) $TEX_{86}$- and RI-OH'-derived SST anomalies using calibrations in Kim et al. (2010) and Lü et al. (2015) as well as $OH^{c}$-derived SST (Fietz et al., 2016). Data and graphs (b–c) adapted from Fietz et al. (2013). Data and graphs (d–f) adapted from Fietz et al. (2016). Blue shaded bars in (d–f) denote glacial stages. All index equations are provided in Table 1. All anomalies refer to the core top value as "0."

OH$^c$ index, the assumed cold-water end-member OH-isoGDGT-0 is subtracted from the numerator (Table 1). The fact that this approach improves the reconstruction of temperature evolution suggests that the addition of OH-isoGDGT in the temperature index may help to fully capture the temperature responses of archaeal membranes to temperature changes in polar waters. The global calibration of RI-OH (Lü et al., 2015) consists of 107 data points, a far cry from the $TEX_{86}$ calibration data set (n >1,000; Tierney and Tingley, 2015). Here, we show that combining recently published surface sediment OH-isoGDGT data (n = 167; Figure 1c) does not change the global calibration equation nor the closeness of fit, but the database should be expanded to improve its robustness. Improvement of both the isoGDGT- and the OH-isoGDGT-based proxy calibrations remains a priority task for the future. As for $TEX_{86}$, one approach is to develop more regional calibrations or use alternative statistical approaches, such as BAYSPAR (Tierney and Tingley, 2014) and OPTiMAL (Eley et al., 2019).

Nonetheless, some uncertainties remain. Even though OH-isoGDGTs have been found in cultured mesophilic Group I Thaumarchaeota and methanogenic Euryarchaeota (X.-L. Liu et al., 2012), and that OH-isoGDGTs have been proposed to be produced autochthonously in the marine water column (Lü et al., 2015; Kaiser and Arz, 2016; Lü et al., 2019; Davtian et al., 2019) and thus may circumvent the impact of terrestrial bias in $TEX_{86}$-reconstructions (Figure 1), the possibility of terrestrial influence has recently been put forward (Kang et al., 2017; Wei et al., 2019). In addition, OH-isoGDGT proxies may also respond to environmental factors other than temperature, such as salinity, the presence of sea ice (Fietz et al., 2013), and/or seasonality (Lü et al., 2019; Wei et al., 2019). More ground truthing in water column and surface sediments, and most importantly culture incubation studies, are needed.

## CONCLUSIONS

Over the last few decades, the $TEX_{86}$ paleothermometer has been used to help reconstruct past changes in sea surface temperatures in the polar regions (e.g., Table 2). However, several caveats exist (Figure 2) and structurally different isoGDGTs have been identified, such as OH-isoGDGTs. More work is needed to shed light on these compounds and the proxies based on them, but a few preliminary studies show that incorporating OH-isoGDGTs in the temperature proxy index may lead to improved reconstructions in the polar oceans. We thus recommend that the OH-isoGDGTs be analyzed simultaneously during standard isoGDGTs analysis, as this multi-proxy approach will increase the robustness of paleotemperature reconstructions.

### REFERENCES


Bale, N.J., M. Palatinszky, W.I.C. Rijpstra, C.W. Herbold, M. Wagner, and J.S. Sinninghe Damsté. 2019. Membrane lipid composition of the moderately thermophilic ammonia-oxidizing archaeon "*Candidatus* Nitrosotenuis uzonensis" at different growth temperatures. *Applied and Environmental Microbiology* 85:e01332-19, https://doi.org/10.1128/AEM.01332-19.

Becquey, S., and R. Gersonde. 2002. Past hydrographic and climatic changes in the Subantarctic Zone of the South Atlantic: The Pleistocene record from ODP Site 1090. *Palaeogeography, Palaeoclimatology. Palaeoecology* 182:221–239. https://doi.org/10.1016/S0031-0182(01)00497-7.

Bijl, P.K., S. Schouten, A. Sluijs, G.-J. Reichart, J.C. Zachos, and H. Brinkhuis. 2009. Early Palaeogene temperature evolution of the southwest Pacific Ocean. *Nature* 461:776–779, https://doi.org/10.1038/nature08399.

Brassell, S., G. Eglinton, I. Marlowe, U. Pflaumann, and M. Sarnthein. 1986. Molecular stratigraphy: A new tool for climatic assessment. *Nature* 320:129–133, https://doi.org/10.1038/320129a0.

Brinkhuis, H., S. Schouten, M.E. Collinson, A. Sluigs, J.S. Sinninghe Damsté, G.R. Dickens, M. Huber, T.M. Cronin, J. Onodera, K. Takahashi, and others. 2006. Episodic fresh surface waters in the Eocene Arctic Ocean. *Nature* 441:606–609, https://doi.org/10.1038/nature04692.

Chen, L.L., J. Liu, and J.S. Wang. 2018. Sources and distribution of tetraether lipids in sediments from the Zhejiang–Fujian coastal mud area, China, over the past 160 years: Implications for paleoclimate change. *Organic Geochemistry* 121:114–125, https://doi.org/10.1016/j.orggeochem.2018.03.010.

Chugunov, A.O., P.E. Volynsky, N.A. Krylov, I.A. Boldyrev, and R.G. Efremov. 2015. Liquid but durable: Molecular dynamics simulations explain the unique properties of archaeal like membranes. *Scientific Reports* 4:7462, https://doi.org/10.1038/srep07462.

Davtian, N., G. Ménot, Y. Fagault, and E. Bard. 2019. Western Mediterranean Sea paleothermometry over the last glacial cycle based on the novel RI-OH index. *Paleoceanography and Paleoclimatology* 34:616–634, https://doi.org/10.1029/2018PA003452.

de Bar, M.W., S.W. Rampen, E.C. Hopmans, J.S. Sinnghe Damsté, and S. Schouten. 2019. Constraining the applicability of organic paleotemperature proxies for the last 90 Myrs. *Organic Geochemistry* 128:122–136, https://doi.org/10.1016/j.orggeochem.2018.12.005.

De Rosa, M., E. Esposito, A. Gambacorta, B. Nicolaus, and J.D. Bu'Lock. 1980. Effects of temperature on ether lipid composition of *Caldariella acidophila*. *Phytochemistry* 19:827–831, https://doi.org/10.1016/0031-9422(80)85120-X.

Eley, Y.L., W. Thompson, S. E. Greene, I. Mandel, K. Edgar, J.A. Bendle, and T. Dunkley Jones. 2019. OPTiMAL: A new machine learning approach for GDGT-based palaeothermometry. *Climate of the Past – Discussion*, https://doi.org/10.5194/cp-2019-60, in review.

Elling, F.J., M. Könneke, J.S. Lipp, K.W. Becker, E.J. Gagen, and K.-U. Hinrichs. 2014. Effects of growth phase on the membrane lipid composition of the thaumarchaeon *Nitrosopumilus maritimus* and their implications for archaeal lipid distributions in the marine environment. *Geochimica et Cosmochimica Acta* 141:579–597, https://doi.org/10.1016/j.gca.2014.07.005.

Elling, F.J., M. Könneke, M. Mußmann, A. Greve, and K.-U. Hinrichs. 2015. Influence of temperature, pH, and salinity on membrane lipid composition and $TEX_{86}$ of marine planktonic thaumarchaeal isolates. *Geochimica et Cosmochimica Acta* 171:238–255, https://doi.org/10.1016/j.gca.2015.09.004.

Elling, F.J., M. Könneke, G.W. Nicol, M. Stieglmeier, B. Bayer, E. Spieck, J.R. de la Torre, K.W. Becker, M. Thomm, J.I. Prosser, and others. 2017. Chemotaxonomic characterisation of the thaumarchaeal lipidome. *Environmental Microbiology* 19:2,681–2,700, https://doi.org/10.1111/1462-2920.13759.

Etourneau, J., L.G. Collins, V. Willmott, J.-H. Kim, L. Barbara, A. Leventer, S. Schouten, J.S. Sinninghe Damsté, A. Bianchini, V. Klein, and others. 2013. Holocene climate variations in the western Antarctic Peninsula: Evidence for sea ice extent predominantly controlled by changes in insolation and ENSO variability. *Climate of the Past* 9:1,431–1,446, https://doi.org/10.5194/cp-9-1431-2013.

Etourneau, J., G. Sgubin, X. Crosta, D. Swingedouw, V. Willmott, L. Barbara, M.-N. Houssais, S. Schouten, J.S. Sinninghe Damsté, H. Goosse, and others. 2019. Ocean temperature impact on ice shelf extent in the eastern Antarctic Peninsula. *Nature Communications* 10:304, https://doi.org/10.1038/s41467-018-08195-6.

Fietz, S., C. Huguet, G. Rueda, B. Hambach, and A. Rosell-Melé. 2013. Hydroxylated isoprenoidal GDGTs in the Nordic seas. *Marine Chemistry* 152:1–10, https://doi.org/10.1016/j.marchem.2013.02.007.

Fietz, S., S.L. Ho, C. Huguet, A. Rosell-Melé, and A. Martínez-García. 2016. Appraising GDGT-based seawater temperature indices in the Southern Ocean. *Organic Geochemistry* 102:93–105, https://doi.org/10.1016/j.orggeochem.2016.10.003.

Gabriel, J.L., and P.L.G. Chong. 2000. Molecular modeling of archaebacterial bipolar tetraether lipid membranes. *Chemistry and Physics of Lipids* 105:193–200, https://doi.org/10.1016/S0009-3084(00)00126-2.

Hansen, J., R. Ruedy, M. Sato, and K. Lo. 2010. Global surface temperature change. *Reviews of Geophysics* 48(4), https://doi.org/10.1029/2010RG000345.

Hartman, J.D., F. Sangiorgi, A. Salabarnada, F. Peterse, A.J.P. Houben, S. Schouten, H. Brinkhuis, C. Escutia, and P.K. Bijl. 2018. Paleoceanography and ice sheet variability offshore Wilkes Land, Antarctica: Part 3. Insights from Oligocene–Miocene $TEX_{86}$-based sea surface temperature reconstructions. *Climate of the Past* 14:1,275–1,297, https://doi.org/10.5194/cp-14-1275-2018.

Hayes, C.T., A. Martínez-García, A.P. Hasenfratz, S.L. Jaccard, D.A. Hodell, D.M. Sigman, G.H. Haug, and R.F. Anderson. 2014. A stagnation event in the deep South Atlantic during the last interglacial period. *Science* 346:1,514–1,517, https://doi.org/10.1126/science.1256620.

Hayes, J.H. 2000. Lipids as a common interest of microorganisms and geochemists. *Proceedings of the National Academy of Sciences of the United States of America* 97:14,033–14,034, https://doi.org/10.1073/pnas.97.26.14033.

Herbert, T.D. 2014. Alkenone paleotemperature determinations. Pp. 399–433 in *Treatise on Geochemistry,* 2nd ed. H.D. Holland and K. Turekian, eds, Elsevier, https://doi.org/10.1016/B978-0-08-095975-7.00615-X.

Hinrichs, K.U., J.M. Hayes, S.P. Sylva, P.G. Brewer, and E.F. DeLong. 1999. Methane consuming archaebacteria in marine sediments. *Nature* 398:802–805, https://doi.org/10.1038/19751.

Ho, S.L., B.D.A. Naafs, and F. Lamy. 2013. Alkenone paleothermometry based on the haptophyte algae. Pp. 755–764 in *The Encyclopedia of Quaternary Science*. S. Elias, ed., Elsevier.

Ho, S.L., G. Mollenhauer, S. Fietz, A. Martínez-Garcia, F. Lamy, G. Rueda, K. Schipper, M. Méheust, A. Rosell-Melé, R. Stein, and R. Tiedemann. 2014. Appraisal of $TEX_{86}$ and $TEX^{L}_{86}$ thermometries in subpolar and polar regions. *Geochimica et Cosmochimica Acta* 131:213–226, https://doi.org/10.1016/j.gca.2014.01.001.

Ho, S.L., and T. Laepple. 2016. Flat meridional temperature gradient in the early Eocene in the subsurface rather than surface ocean. *Nature Geoscience* 9:606–610, https://doi.org/10.1038/ngeo2763.

Hopmans, E.C., J.W.H. Weijers, E. Schefuß, L. Herfort, J.S. Sinninghe Damsté, and S. Schouten. 2004. A novel proxy for terrestrial organic matter in sediments based on branched and isoprenoid tetraether lipids. *Earth and Planetary Science Letters* 224(1–2):107–116, https://doi.org/10.1016/j.epsl.2004.05.012.

Huguet, C., A. Schimmelmann, R. Thunell, L.J. Lourens, J.S. Sinninghe Damsté, and S. Schouten. 2007. A study of the $TEX_{86}$ paleothermometer in the water column and sediments of the Santa Barbara Basin, California. *Paleoceanography and Paleoclimatology* 22(3), https://doi.org/10.1029/2006PA001310.

Huguet, C., G.J. de Lange, Ö. Gustafsson, J.J. Middelburg, J.S. Sinninghe Damsté, and S. Schouten. 2008. Selective preservation of soil organic matter in oxidized marine sediments (Madeira Abyssal Plain). *Geochimica et Cosmochimica Acta* 72:6,061–6,068, https://doi.org/10.1016/j.gca.2008.09.021.

Huguet, C., S. Fietz, and A. Rosell-Melé. 2013. Global distribution patterns of hydroxy glycerol dialkyl glycerol tetraethers. *Organic Geochemistry* 57:107–118, https://doi.org/10.1016/j.orggeochem.2013.01.010.

Huguet, C., S. Fietz, A. Rosell-Melé, X. Daura, and L. Costenaro. 2017. Molecular dynamics simulation study of the effect of glycerol dialkyl glycerol tetraether hydroxylation on membrane thermostability. *Biochimica et Biophysica Acta (BBA) – Biomembranes* 1859(5):966–974, https://doi.org/10.1016/j.bbamem.2017.02.009.

Hurley, S.J., F.J. Elling, M. Könneke, C. Buchwald, S.C. Wankel, A.E. Santoro, J.S. Lipp, K.-U. Hinrichs, and A. Pearson. 2016. Influence of ammonia oxidation rate on thaumarchaeal lipid composition and the $TEX_{86}$ temperature proxy. *Proceedings of the National Academy of Sciences of the United States of America* 113:7,762–7,767, https://doi.org/10.1073/pnas.1518534113.

IPCC (Intergovernmental Panel on Climate Change). 2019. *Special Report on the Ocean and Cryosphere in a Changing Climate*. H.-O. Pörtner, D.C. Roberts, V. Masson-Delmotte, P. Zhai, M. Tignor, E. Poloczanska, K. Mintenbeck, A. Alegría, M. Nicolai, A. Okem, J. Petzold, B. Rama, and N.M. Weyer, eds, https://www.ipcc.ch/site/assets/uploads/sites/3/2019/12/02_SROCC_FM_FINAL.pdf.

Ionescu, D., S. Penno, M. Haimovich, B. Rihtman, A. Goodwin, D. Schwartz, L. Hazanov, M. Chernihovsky, A.F. Post, and A. Oren. 2009. Archaea in the Gulf of Aqaba. *FEMS Microbiology Letters* 69:425–438, https://doi.org/10.1111/j.1574-6941.2009.00721.x.

Jacob, T.J. Wahr, W.T. Pfeffer, and S. Swenson. 2012. Recent contributions of glaciers and ice caps to sea level rise. *Nature* 482:514–518, https://doi.org/10.1038/nature10847.

Jenkyns, H.C., A. Forster, S. Schouten, and J.S. Sinninghe Damsté. 2004. High temperatures in the Late Cretaceous Arctic Ocean. *Nature* 432:888–892, https://doi.org/10.1038/nature03143.

Jenkyns, H.C., L. Schouten-Huibers, S. Schouten, and J.S. Sinninghe Damsté. 2012. Warm Middle Jurassic–Early Cretaceous high-latitude sea-surface temperatures from the Southern Ocean. *Climate of the Past* 8:215–226, https://doi.org/10.5194/cp-8-215-2012.

Kaiser, J., and H.W. Arz. 2016. Sources of sedimentary biomarkers and proxies with potential paleoenvironmental significance for the Baltic Sea. *Continental Shelf Research* 122:102–119, https://doi.org/10.1016/j.csr.2016.03.020.

Kang, S., K.H. Shin, and J.H. Kim. 2017. Occurrence and distribution of hydroxylated isoprenoid glycerol dialkyl glycerol tetraethers (OH-GDGTs) in the Han River system, South Korea. *Acta Geochimica* 36:367–369, https://doi.org/10.1007/s11631-017-0165-3.

Kim, J.-H., S. Schouten, E.C. Hopmans, B. Donner, and J.S. Sinninghe Damsté. 2008. Global sediment core-top calibration of the $TEX_{86}$ paleothermometer in the ocean. *Geochimica et Cosmochimica Acta* 72:1,154–1,173, https://doi.org/10.1016/j.gca.2007.12.010.

Kim, J.-H., X. Crosta, E. Michel, S. Schouten, J. Duprat, and J.S. Sinninghe Damsté. 2009. Impact of lateral transport on organic proxies in the Southern Ocean. *Quaternary Research* 71:246–250, https://doi.org/10.1016/j.yqres.2008.10.005.

Kim, J.-H., J. van der Meer, S. Schouten, P. Helmke, V. Willmott, F. Sangiorgi, N. Koç, E.C. Hopmans, and J.S. Sinninghe Damsté. 2010. New indices and calibrations derived from the distribution of crenarchaeal isoprenoid tetraether lipids: Implications for past sea surface temperature reconstructions. *Geochimica et Cosmochimica Acta* 74:4,639–4,654, https://doi.org/10.1016/j.gca.2010.05.027.

Kim, J.-H., X. Crosta, V. Willmott, H. Renssen, G. Masse, J. Bonnin, P. Helmke, S. Schouten, and J.S. Sinninghe Damsté. 2012. Holocene subsurface temperature variability in the eastern Antarctic continental margin. *Geophysical Research Letters* 39:L06705, https://doi.org/10.1029/2012GL051157.

Knies, J., P. Cabedo-Sanz, S.T. Belt, S. Baranwa, S. Fietz, and A. Rosell-Melé. 2014. The emergence of modern sea ice cover in the Arctic Ocean. *Nature Communications* 5:5608, https://doi.org/10.1038/ncomms6608.

Koga, Y., and H. Morii. 2007. Biosynthesis of ether-type polar lipids in archaea and evolutionary considerations. *Microbiology and Molecular Biology Reviews* 71:97–120, https://doi.org/10.1128/MMBR.00033-06.

Konings, W.N., S.V. Albers, S. Koning, and A.J.M. Driessen. 2002. The cell membrane plays a crucial role in survival of bacteria and archaea in extreme environments. *Antonie Van Leeuwenhoek* 81:61–72, https://doi.org/10.1023/A:1020573408652.

Kremer, A., R. Stein, K. Fahl, Z. Ji, Z. Yang, S. Wiers, J. Matthiessen, M. Forwick, L. Löwemark, M. O'Regan, J. Chen, and I. Snowball. 2018. Changes in sea ice cover and ice sheet extent at the Yermak Plateau during the last 160 ka: Reconstructions from biomarker records. *Quaternary Science Reviews* 182:93–108, https://doi.org/10.1016/j.quascirev.2017.12.016.

Levy R., D. Harwood, F. Florindo, F. Sangiorgi, R. Tripati, H. von Eynatten, E. Gasson, G. Kuhn, A. Tripati, R. DeConto, and others. 2016. Antarctic ice sheet sensitivity to atmospheric $CO_2$ variations in the early to mid-Miocene. *Proceedings of the National Academy of Sciences of the United States of America* 113:3,453–3,458, https://doi.org/10.1073/pnas.1516030113.

Lipp, J.S., and K.-U. Hinrichs. 2009. Structural diversity and fate of intact polar lipids in marine sediments. *Geochimica et Cosmochimica Acta* 73:6,816–6,833, https://doi.org/10.1016/j.gca.2009.08.003.

Lisiecki, L.E., and M.E. Raymo. 2005. A Pliocene-Pleistocene stack of 57 globally distributed benthic $\delta^{18}O$ records. *Paleoceanography* 20(1), https://doi.org/10.1029/2004PA001071.

Liu, X-.L., J.S. Lipp, J.H. Simpson, Y.-S. Lin, R.E. Summons, and K.-U. Hinrichs. 2012. Mono- and dihydroxyl glycerol dibiphytanyl glycerol tetraethers in marine sediments: Identification of both core and intact polar lipid forms. *Geochimica et Cosmochimica Acta* 89:102–115, https://doi.org/10.1016/j.gca.2012.04.053.

Liu, Z., M. Pagani, D. Zinniker, R. DeConto, M. Huber, H. Brinkhuis, S.R. Shah, R.M. Leckie, and A. Pearson. 2009. Global cooling during the Eocene-Oligocene climate transition. *Science* 323:1,187–1,190, https://doi.org/10.1126/science.1166368.

Locarnini, R.A., A.V. Mishonov, J.I. Antonov, T.P. Boyer, H.E. Garcia, O.K. Baranova, M.M. Zweng, C.R. Paver, J.R. Reagan, D.R. Johnson, and others. 2013. World Ocean Atlas 2013, Volume 1: Temperature. S. Levitus, ed., A. Mishonov, tech. ed., NOAA Atlas NESDIS 73, 40 pp.

Lü, X., X.-L. Liu, F.J. Elling, H. Yang, S. Xie, J. Song, X. Li, H. Yuan, N. Li, and K.U. Hinrichs. 2015. Hydroxylated isoprenoid GDGTs in Chinese coastal seas and their potential as a paleotemperature proxy for mid-to-low latitude marginal seas. *Organic Geochemistry* 89–90:31–43, https://doi.org/10.1016/j.orggeochem.2015.10.004.

Lü, X., J. Chen, T. Han, H. Yang, W. Wu, W. Ding, and K.U. Hinrichs. 2019. Origin of hydroxyl GDGTs and regular isoprenoid GDGTs in suspended particulate matter of Yangtze River Estuary. *Organic Geochemistry* 128:78–85, https://doi.org/10.1016/j.orggeochem.2018.12.010.

Martínez-García, A., A. Rosell-Melé, W. Geibert, R. Gersonde, P. Masqué, V. Gaspari, and C. Barbante. 2009. Links between iron supply, marine productivity, sea surface temperatures and

$CO_2$ over the last 1.1 Ma. *Paleoceanography and Paleoclimatology* 24(1), https://doi.org/10.1029/2008PA001657.

McKay, R., T. Naish, L. Carter, C. Riesselman, R. Dunbar, C. Sjunneskog, D. Winter, F. Sangiorgi, C. Warren, M. Pagani, and others. 2012. Antarctic and Southern Ocean influences on Late Pliocene global cooling. *Proceedings of the National Academy of Sciences of the United States of America* 109:6,423–6,428, https://doi.org/10.1073/pnas.1112248109.

Mulvaney, R., N. Abram, R. Hindmarsh, C. Arrowsmith, L. Fleet, J. Triest, L.C. Sime, O. Alemany, and S. Foord. 2012. Recent Antarctic Peninsula warming relative to Holocene climate and ice-shelf history. *Nature* 489:141–144, https://doi.org/10.1038/nature11391.

Oger, P.M., and A. Cario. 2013. Adaptation of the membrane in Archaea. *Biophysical Chemistry* 183:42–56, https://doi.org/10.1016/j.bpc.2013.06.020.

Park, E., J. Hefter, G. Fischer, M. Iversen, S. Ramondenc, E.M. Nöthig, and G. Mollenhauer. 2019. Seasonality of archaeal lipid flux and GDGT-based thermometry in sinking particles of high latitude regions: Fram Strait (79°N) and Antarctic Polar Front (50°S). *Biogeosciences* 16:2,247–2,268, https://doi.org/10.5194/bg-2019-34.

Park, Y., M. Yamamoto, S. Nam, T. Irino, L. Polyak, N. Harada, K. Nagashima, B. Khim, K. Chikita, and S. Saitoh. 2014. Distribution, source and transportation of glycerol dialkyl glycerol tetraethers in surface sediments from the western Arctic Ocean and the northern Bering Sea. *Marine Chemistry* 165:10–24, https://doi.org/10.1016/j.marchem.2014.07.001.

Pearson, A., and A.E. Ingalls. 2013. Assessing the use of archaeal lipids as marine environmental proxies. *Annual Review of Earth and Planetary Sciences* 41:359–384, https://doi.org/10.1146/annurev-earth-050212-123947.

Qin, W., L.T. Carlson, E.V. Armbrust, A.H. Devol, J.W. Moffett, D.A. Stahl, and A.E. Ingalls. 2015. Confounding effects of oxygen and temperature on the $TEX_{86}$ signature of marine Thaumarchaeota. *Proceedings of the National Academy of Sciences of the United States of America* 112:10,979–10,984, https://doi.org/10.1073/pnas.1501568112.

Ren, Q., and I.T. Paulsen. 2005. Comparative analyses of fundamental differences in membrane transport capabilities in prokaryotes and eukaryotes. *PLoS Computational Biology* 1:e27, https://doi.org/10.1371/journal.pcbi.0010027.

Rintoul, S.R., S.L. Chown, R.M. DeConto, M.H. England, H.A. Fricker, V. Masson-Delmotte, T.R. Naish, M.J. Siegert, and J.C. Xavier. 2018. Choosing the future of Antarctica. *Nature* 558:233–241, https://doi.org/10.1038/s41586-018-0173-4.

Rueda, G., S. Fietz, and A. Rosell-Melé. 2013. Coupling of air and sea surface temperatures in the eastern Fram Strait during the last 2000 years. *The Holocene* 23:692–698, https://doi.org/10.1177/0959683612470177.

Sangiorgi, F., P.K. Bijl, S. Passchier, U. Salzmann, S. Schouten, R. McKay, R.D. Cody, J. Pross, T. van de Flierdt, S.M. Bohaty, and others. 2018. Southern Ocean warming and Wilkes Land ice sheet retreat during the mid-Miocene. *Nature Communications* 9:317, https://doi.org/10.1038/s41467-017-02609-7.

Schlitzer, R. 2018. Ocean Data View, Version 5.1.0, https://odv.awi.de.

Schouten, S., E.C. Hopmans, E. Schefuß, and J.S. Sinninghe Damsté. 2002. Distributional variations in marine crenarchaeotal membrane lipids: A new tool for reconstructing ancient sea water temperatures? *Earth and Planetary Science Letters* 204:265–274, https://doi.org/10.1016/S0012-821X(02)00979-2.

Schouten, S., E.C. Hopmans, and J.S. Sinninghe Damsté. 2013. The organic geochemistry of glycerol dialkyl glycerol tetraether lipids: A review. *Organic Geochemistry* 54:19–61, https://doi.org/10.1016/j.orggeochem.2012.09.006.

Shah, S.R., G. Mollenhauer, N. Ohkouchi, T.I. Eglinton, and A. Pearson. 2008. Origins of archaeal tetraether lipids in sediments: Insights from radiocarbon analysis. *Geochimica et Cosmochimica Acta* 72:4,577–4,594, https://doi.org/10.1016/j.gca.2008.06.021.

Shafiee, R.T., J.T. Snow, Q. Zhang, and R.E.M. Rickaby. 2019. Iron requirements and uptake strategies of the globally abundant marine ammonia-oxidising archaeon, *Nitrosopumilus maritimus* SCM1. *The ISME Journal* 13:2,295–2,305, https://doi.org/10.1038/s41396-019-0434-8.

Shevenell, A.E., A.E. Ingalls, E.W. Domack, and C. Kelly. 2011. Holocene Southern Ocean surface temperature variability west of the Antarctic Peninsula. *Nature* 470:250–254, https://doi.org/10.1038/nature09751.

Sinninghe Damsté, J.S., S. Schouten, E.C. Hopmans, A.C. van Duin, and J.A. Geenevasen. 2002. Crenarchaeol: The characteristic core glycerol dibiphytanyl glycerol tetraether membrane lipid of cosmopolitan pelagic crenarchaeota. *Journal of Lipid Research* 43:1,641–1,651, https://doi.org/10.1194/jlr.M200148-JLR200.

Sluijs, A., S. Schouten, M. Pagani, M. Woltering, H. Brinkhuis, J.S. Sinninghe Damsté, G.R. Dickens, M. Huber, G.-J. Reichart, R. Stein, and others. 2006. Subtropical Arctic Ocean temperatures during the Palaeocene/Eocene thermal maximum. *Nature* 441:610–613, https://doi.org/10.1038/nature04668.

Spielhagen, R.F., K. Werner, S.A. Sørensen, K. Zamelczyk, E. Kandiano, G. Budeus, K. Husum, T.M. Marchitto, and M. Hald. 2011. Enhanced modern heat transfer to the Arctic by warm Atlantic water. *Science* 331:450–453, https://doi.org/10.1126/science.1197397.

Tierney, J.E. 2014. Biomarker-based inferences of past climate: The $TEX_{86}$ paleotemperature proxy. Pp. 379–393 in *Treatise on Geochemistry,* 2nd ed. H.D. Holland, K.K. Turekian, eds, Elsevier, https://doi.org/10.1016/B978-0-08-095975-7.01032-9.

Tierney, J.E., and M.P. Tingley. 2014. A Bayesian, spatially-varying calibration model for the $TEX_{86}$ proxy. *Geochimica et Cosmochimica Acta* 127:83–106, https://doi.org/10.1016/j.gca.2013.11.026.

Tierney, J.E., and M.P. Tingley. 2015. A $TEX_{86}$ surface sediment database and extended Bayesian calibration. *Scientific Data* 2:150029, https://doi.org/10.1038/sdata.2015.29.

Trommer, G., M. Siccha, M.T. van der Meer, S. Schouten, J.S. Sinninghe Damsté, H. Schulz, C. Hemleben, and M. Kucera. 2009. Distribution of Crenarchaeota tetraether membrane lipids in surface sediments from the Red Sea. *Organic Geochemistry* 40:724–731, https://doi.org/10.1016/j.orggeochem.2009.03.001.

Wei, B., G. Jia, J. Hefter, M. Kang, E. Park, and G. Mollenhauer. 2019. Comparison of the $U^{K'}_{37}$, LDI, $TEX^{H}_{86}$ and RI-OH temperature proxies in the northern shelf of the South China Sea. *Biogeosciences-Discussion*, https://doi.org/10.5194/bg-2019-345, in review.

Wuchter, C., S. Schouten, M.J.L. Coolen, and J.S. Sinninghe Damsté. 2004. Temperature-dependent variation in the distribution of tetraether membrane lipids of marine Crenarchaeota: Implications for $TEX_{86}$ paleothermometry. *Paleoceanography and Paleoclimatology* 19(4), https://doi.org/10.1029/2004PA001041.

Zhang, Y.G., M. Pagani, and Z. Wang. 2016. Ring Index: A new strategy to evaluate the integrity of $TEX_{86}$ paleothermometry. *Paleoceanography and Paleoclimatology* 31:220–232, https://doi.org/10.1002/2015PA002848.

Zhou, A., Y. Weber, B.K. Chiu, F.J. Elling, A.B. Cobban, A. Pearson, and W.D. Leavitt. 2020. Energy flux controls tetraether lipid cyclization in *Sulfolobus acidocaldarius*. *Environmental Microbiology* 22:343–353, https://doi.org/10.1111/1462-2920.14851.

Zonneveld, K.A., G.J. Versteegh, S. Kasten, T.I. Eglington, K.-C. Emeis, C. Huguet, B.P. Koch, G.J. de Lange, J.W. de Leeuw, J.J. Middelburg, and others. 2010. Selective preservation of organic matter in marine environments: Processes and impact on the sedimentary record. *Biogeosciences* 7:483–511, https://doi.org/10.5194/bg-7-483-2010.

Zamelczyk, K., T.L. Rasmussen, K. Husum, H. Haflidason, A. de Vernal, E. K. Ravna, M. Hald, and C. Hillaire-Marcel. 2012. Paleoceanographic changes and calcium carbonate dissolution in the central Fram Strait during the last 20 ka. *Quaternary Research* 78:405–416, https://doi.org/10.1016/j.yqres.2012.07.006.

## ACKNOWLEDGMENTS

The authors thank two anonymous reviewers and guest editor Amelia Shevenell for the thorough review and valuable comments and suggestions. This work is based on the research supported by the National Research Foundation (NRF) of South Africa awarded to SF (#93072, #98905, #110731). CH wishes to acknowledge the Los Andes Faculty of Science INV-2019-84-1814 and the Humboldt Research Fellowship for Experienced Researchers. SLH acknowledges funding from the Ministry of Science and Technology (Taiwan; # 107-2611-M-002-021-MY3).

## AUTHORS

**Susanne Fietz** (sfietz@sun.ac.za) is Senior Lecturer, Department of Earth Sciences, Stellenbosch University, Stellenbosch, South Africa. **Sze Ling Ho** is Assistant Professor, National Taiwan University, Taipei, Taiwan. **Carme Huguet** is Associate Professor, Geoscience Department, Universidad de los Andes, Bogotá, Colombia.

## AUTHOR CONTRIBUTIONS

All authors contributed equally to this article.

## ARTICLE CITATION

Fietz, S., S.L. Ho, and C. Huguet. 2020. Archaeal membrane lipid-based paleothermometry for applications in polar oceans. *Oceanography* 33(2):104–114, https://doi.org/10.5670/oceanog.2020.207.

## COPYRIGHT & USAGE